

TECHNICAL REPORT HL-92-9

# DEPTH-AVERAGED NUMERICAL MODELING FOR CURVED CHANNELS

by

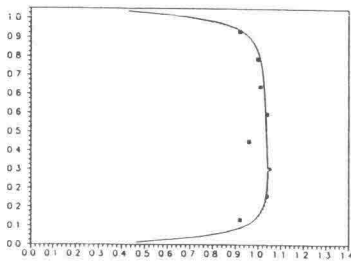
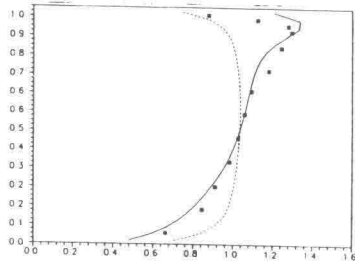
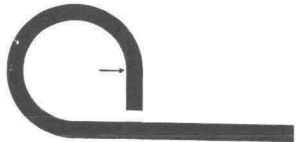
Robert S. Bernard, Michael L. Schneider

Hydraulics Laboratory

DEPARTMENT OF THE ARMY  
Waterways Experiment Station, Corps of Engineers  
3909 Halls Ferry Road, Vicksburg, Mississippi 39180-6199



US Army Corps  
of Engineers



September 1992

Final Report

Approved For Public Release; Distribution Is Unlimited

Prepared for DEPARTMENT OF THE ARMY  
US Army Corps of Engineers  
Washington, DC 20314-1000

Under Civil Works Investigation Work Unit 32542

HYDRAULICS  
LABORATORY

Destroy this report when no longer needed. Do not return  
it to the originator.

The findings in this report are not to be construed as an official  
Department of the Army position unless so designated  
by other authorized documents.

The contents of this report are not to be used for  
advertising, publication, or promotional purposes.  
Citation of trade names does not constitute an  
official endorsement or approval of the use of  
such commercial products.

# REPORT DOCUMENTATION PAGE

*Form Approved*  
OMB No. 0704-0188

Public reporting burden for this collection of information is estimated to average 1 hour per response, including the time for reviewing instructions, searching existing data sources, gathering and maintaining the data needed, and completing and reviewing the collection of information. Send comments regarding this burden estimate or any other aspect of this collection of information, including suggestions for reducing this burden, to Washington Headquarters Services, Directorate for Information Operations and Reports, 1215 Jefferson Davis Highway, Suite 1204, Arlington, VA 22202-4302, and to the Office of Management and Budget, Paperwork Reduction Project (0704-0188), Washington, DC 20503.

<b>1. AGENCY USE ONLY (Leave blank)</b>	<b>2. REPORT DATE</b> September 1992	<b>3. REPORT TYPE AND DATES COVERED</b> Final report
---	---	---

<b>4. TITLE AND SUBTITLE</b>  Depth-Averaged Numerical Modeling for Curved Channels	<b>5. FUNDING NUMBERS</b>  WU 32542
---	---

<b>6. AUTHOR(S)</b>  Robert S. Bernard and Michael L. Schneider	
---	--

<b>7. PERFORMING ORGANIZATION NAME(S) AND ADDRESS(ES)</b>  USAE Waterways Experiment Station, Hydraulics Laboratory, 3909 Halls Ferry Road, Vicksburg, MS 39180-6199	<b>8. PERFORMING ORGANIZATION REPORT NUMBER</b>  Technical Report HL-92-9
--	---

<b>9. SPONSORING/MONITORING AGENCY NAME(S) AND ADDRESS(ES)</b>  US Army Corps of Engineers, Washington, DC 20314-1000	<b>10. SPONSORING/MONITORING AGENCY REPORT NUMBER</b>
---	---

**11. SUPPLEMENTARY NOTES**  
Available from National Technical Information Service, 5285 Port Royal Road, Springfield, VA 22161.

<b>12a. DISTRIBUTION / AVAILABILITY STATEMENT</b>  Approved for public release; distribution is unlimited.	<b>12b. DISTRIBUTION CODE</b>
--	-------------------------------

**13. ABSTRACT (Maximum 200 words)**

Without some correction for the interaction between lateral curvature and vertically nonuniform velocity, depth-averaged numerical models cannot predict the gradual migration of high velocity toward the outside of channel bends. Conventional depth-averaging does not account for the curvature-induced secondary flow that gives rise to the migration. To remedy this deficiency, a secondary flow correction (SFC) has been developed and incorporated in the two-dimensional STREMR code. The secondary governing equation contains two empirical coefficients, and these have been adjusted to make STREMR predictions agree with observed velocity profiles for a single 270-deg bend. Without further adjustment, the SFC yields comparable accuracy for multiple-bend predictions in two other channels with depth, curvature, and bottom friction different from the 270-deg case. This suggests that the SFC may be useful in general for bendways with small curvature, gentle side slope, and moderate bottom friction.

<b>14. SUBJECT TERMS</b> Bendway                      Secondary flow Numerical model            Turbulence Open channel                Velocity distribution	<b>15. NUMBER OF PAGES</b> 46
	<b>16. PRICE CODE</b>

<b>17. SECURITY CLASSIFICATION OF REPORT</b> UNCLASSIFIED	<b>18. SECURITY CLASSIFICATION OF THIS PAGE</b> UNCLASSIFIED	<b>19. SECURITY CLASSIFICATION OF ABSTRACT</b>	<b>20. LIMITATION OF ABSTRACT</b>
--	---	--	-----------------------------------

## PREFACE

The work reported herein was done from October 1990 through August 1991 at the US Army Engineer Waterways Experiment Station (WES) for Headquarters, US Army Corps of Engineers (HQUSACE), as part of the Civil Works Research and Development Program. Funds were allotted under Civil Works Investigation Work Unit 32542, "River Bend System Hydraulics - Imposed Force Component," for which the HQUSACE Program Monitor was Mr. Tom Munsey.

Dr. Robert S. Bernard and Mr. Michael L. Schneider conducted this research and model development under the general supervision of Messrs. Frank A. Herrmann, Director, Hydraulics Laboratory (HL); Richard A. Sager, Assistant Director, HL; Glenn A. Pickering, Chief, Hydraulic Structures Division; and Dr. Jeffery P. Holland, Chief, Reservoir Water Quality Branch. Professor Gary Parker and Dr. Helgi Johannesson, University of Minnesota, provided valuable technical advice prior to the investigation.

At the time of publication of this report, Director of WES was Dr. Robert W. Whalin. Commander and Deputy Director was COL Leonard G. Hassell, EN.

## CONTENTS

	<u>Page</u>
PREFACE.....	1
CONVERSION FACTORS, NON-SI TO SI (METRIC)	
UNITS OF MEASUREMENT.....	3
PART I:    INTRODUCTION.....	4
PART II:   PRIMARY FLOW.....	6
PART III:  SECONDARY FLOW CORRECTION.....	10
PART IV:   RESULTS.....	14
270-Deg Bendway.....	14
Channel Bend Facility.....	19
Riprap Test Facility.....	20
Hypothetical Effect of Bend Angle.....	27
PART V:   CONCLUSIONS AND RECOMMENDATIONS.....	41
REFERENCES.....	42
APPENDIX A:  NOTATION.....	A1

CONVERSION FACTORS, NON-SI TO SI (METRIC)  
UNITS OF MEASUREMENT

Non-SI units of measurement used in this report can be converted to SI  
(metric) units as follows:

<u>Multiply</u>	<u>By</u>	<u>To Obtain</u>
cubic feet	0.02831685	cubic metres
degrees (angle)	0.01745329	radians
feet	0.3048	metres

DEPTH-AVERAGED NUMERICAL MODELING  
FOR CURVED CHANNELS

PART I: INTRODUCTION

Genuinely two-dimensional (2-D) flows are uncommon in hydraulics, but depth-averaged 2-D models have been widely used for shallow water. One shortcoming of such models is that they fare poorly in channels with significant curvature. This is due to the models' inability to account for the effects of helical secondary flow, which is a three-dimensional (3-D) phenomenon that cannot be represented by conventional depth averaging.

When the depth-averaged streamlines are curved, and the vertical distribution of velocity is nonuniform, centrifugal forces create a torque that generates helicity in the flow. (This is like a screw advancing or retreating in the streamwise direction.) If no correction is added for the secondary flow, depth-averaged models will usually constrain the largest velocities to lie near the inside of a channel bend, instead of allowing the observed gradual migration of high velocity toward the outside.

The influence of secondary flow is well-known for natural meandering channels, where it alters the depth-averaged flow and ultimately the bed itself. In the past this has been simulated with both analytical (closed-form) and numerical (discrete) models. Especially noteworthy among the analytical models is the work of Johannesson and Parker (1989a), who developed equations for predicting velocity redistribution in meandering rivers (1989b). Their success arises from two important model features. First, a perturbation expansion was used to derive a differential equation for the secondary flow from the 3-D equations of motion (with an empirical shape function for the vertical distribution of primary velocity). The differential equation was accurate only to first order, but its closed-form solution offered a credible representation of the secondary flow for small curvature (large radius). Second, by accounting for the rapid attenuation of all velocity components near channel sidewalls, the model reproduced the velocity redistribution observed in channels with uniform width and variable curvature.

Depth-averaged 2-D models such as the STREMR code (Bernard 1989, 1992) are often employed for shallow channels with irregular lateral boundaries as well as nonuniform depth and curvature. This kind of variability makes it

impractical to seek a closed-form solution to the Johannesson-Parker equation for secondary flow, and it may even stretch the applicability of the equation itself. For 2-D models that seek only to calculate the depth-averaged primary flow, however, the overall effect of the secondary flow is more important than its actual structure. In practice it may be sufficient to solve an empirical transport equation for streamwise vorticity that reproduces the depth-averaged influence of the secondary flow, but not necessarily the underlying details. This assumption is the basis for the approach taken herein.

From qualitative arguments concerning the interaction of lateral curvature, bottom friction, and vertical nonuniformity, one can establish a plausible form for an equation that governs the production, transport, and dissipation of streamwise vorticity (helical secondary flow). The latter creates a shear stress in the vertical plane, parallel to the primary direction of flow. Sidewalls and variations in depth cause lateral nonuniformity of this stress, which transports momentum in the lateral direction and alters the distribution of depth-averaged velocity. Empirical coefficients allow the equations to be tuned for quantitative agreement with experimental data. If the model is to be truly useful for making predictions, then the empirical coefficients must be universal; i.e., one set of values should be adequate for all channel configurations of interest.

This report documents the empirical development and implementation of a secondary flow correction (SFC) for the 2-D STREMR code. Part II discusses the depth-averaged equations for the primary flow and the  $k-\epsilon$  turbulence model, and Part III presents arguments used in the formulation of the SFC. Part IV offers a comparison of computed and measured results for three different bendway configurations, and Part V summarizes the conclusions and recommendations for this study.

PART II: PRIMARY FLOW

The governing equations for the primary 2-D flow are the depth-averaged, incompressible Navier-Stokes equations. These are the equations for conservation of mass and momentum, given respectively by

$$\nabla \cdot (h\mathbf{u}) = 0 \quad (1)$$

$$\frac{\partial \mathbf{u}}{\partial t} + \mathbf{u} \times \nabla \mathbf{u} = \mathbf{T} - \mathbf{X} + \mathbf{S} - \frac{\nabla p}{\rho} \quad (2)$$

where

$\nabla$  = gradient operator

$\mathbf{u}$  = velocity

$t$  = time

$\mathbf{T}$  = viscous force arising from the depth-averaged stress tensor

$\mathbf{X}$  = bottom-friction force

$\mathbf{S}$  = force arising from secondary flow

$p$  = pressure

$\rho$  = density

In the above equations, an underline indicates a vector. The cartesian x- and y-components of  $\mathbf{T}$  are, respectively

$$T_1 = h^{-1} \nu \nabla \cdot (h \nabla u) + 2\nu_x u_x + \nu_y (u_y + v_x) \quad (3)$$

$$T_2 = h^{-1} \nu \nabla \cdot (h \nabla v) + 2\nu_y v_y + \nu_x (v_x + u_y) \quad (4)$$

where  $u$  and  $v$  are the x- and y-components of  $\mathbf{u}$ , and the subscripts  $x$  and  $y$  indicate spatial derivatives. The quantity  $\nu$  is the eddy viscosity, which is a kinematic viscosity that is used to represent the influence of small-scale turbulence. It is related to the turbulence energy  $k$  and the turbulence dissipation rate  $\epsilon$  by

$$\nu = C_\nu \frac{k^2}{\epsilon} \quad (5)$$

where  $C_\nu$  is a dimensionless empirical coefficient.

The streamwise deceleration  $\mathbf{X}$  due to bottom friction is represented in STREMR by

$$\underline{X} = C_f h^{-1} \underline{u} |\underline{u}| \quad (6)$$

where  $C_f$  is the friction factor given by Manning's equation,

$$C_f = 9.81 n^2 h^{-1/3} \quad (7)$$

and the quantity  $n$  is Manning's coefficient. The value of 9.81 for the constant of proportionality applies only when  $h$  is given in metres. If  $h$  is given in feet, this value becomes 14.5 instead.

The streamwise acceleration  $\underline{S}$  arises from nonuniformity in the depth-averaged shear stress  $\tau_s$  created by the secondary flow. This is given approximately by

$$\underline{S} \approx \rho^{-1} \frac{\underline{u}}{|\underline{u}|} \left[ h^{-1} \underline{n} \cdot \nabla (h \tau_s) + 2 r^{-1} \tau_s \right] \quad (8)$$

where  $\underline{n}$  is a unit vector normal to  $\underline{u}$ , and  $r$  is the lateral radius of curvature, which is related to the velocity and its derivatives by

$$r = \frac{|\underline{u}|^3}{uv(v_y - u_x) + u^2 v_x - v^2 u_y} \quad (9)$$

The operator  $\underline{n} \cdot \nabla (h \tau_s)$  is the normal derivative of the depth-integrated shear stress created by the secondary flow,

$$\underline{n} \cdot \nabla (h \tau_s) = \frac{v(h \tau_s)_x - u(h \tau_s)_y}{|\underline{u}|} \quad (10)$$

The  $k$ - $\epsilon$  turbulence model (Launder and Spalding 1974) provides semi-empirical governing equations for  $k$  and  $\epsilon$ ,

$$\frac{\partial k}{\partial t} + \underline{u} \cdot \nabla k = \nu \Gamma - \epsilon + \sigma_k^{-1} h^{-1} \nabla \cdot (h \nu \nabla k) \quad (11)$$

$$\frac{\partial \epsilon}{\partial t} + \underline{u} \cdot \nabla \epsilon = c_1 \nu \Gamma \frac{\epsilon}{k} - c_2 \frac{\epsilon^2}{k} + \sigma_\epsilon^{-1} h^{-1} \nabla \cdot (h \nu \nabla \epsilon) \quad (12)$$

In Equations 11 and 12, the second term on the left is the advection term. The second and third terms on the right are the dissipation and diffusion terms, respectively. The first term on the right is the production term, which is proportional to

$$\Gamma = 2(u_x^2 + v_y^2) + (u_y + v_x)^2 \quad (13)$$

In this context, advection means transport by the primary flow; production means creation of small-scale turbulence from the primary flow; dissipation means frictional loss through the smallest eddies of the turbulence; and diffusion means the spreading that occurs because of eddy viscosity. The standard set of dimensionless empirical coefficients (Patel, Rodi, and Scheurer 1985) is

$$C_\nu = 0.09$$

$$c_1 = 1.44$$

$$c_2 = 1.92$$

$$\sigma_k = 1.0$$

$$\sigma_\epsilon = 1.3$$

With suitable boundary conditions for  $u$ ,  $v$ ,  $p$ ,  $k$ , and  $\epsilon$ , and with suitable approximations for  $\underline{X}$  and  $\underline{S}$ , Equations 1, 2, 11, and 12 are sufficient for calculating depth-averaged primary flow within the limitations of the  $k$ - $\epsilon$  turbulence model and the definitions for  $\underline{X}$  and  $\underline{S}$ .

In the STREMR code, velocity components normal to the boundaries are held fixed on inlets and solid walls, and computed by a discrete radiation condition (Orlanski 1976) at the outlets. The total flow rate remains constant, as do the individual flow rates through each continuous inlet and outlet. In a given time-step, the velocity normal to any boundary segment is either constant (for inlets and solid walls) or determined by neighboring velocities in the previous time-step (for outlets). For calculating vorticity and shear stress on sidewalls, tangential velocity is assumed proportional to the 1/7 power of distance from the walls.

The value of  $k$  is fixed at a small fraction (0.006) of the primary inflow energy at inlets, and the normal derivative of  $k$  is set to zero at outlets. This estimate for the inflow turbulence energy (whose actual value is unknown) may be somewhat low, but the error has little effect downstream because  $k$  grows rapidly with the developing flow. On the sidewalls,  $k$  is assumed proportional to the 1/7 power of distance from the walls. The normal derivative of  $\epsilon$  is set to zero on all boundaries except inlets, where the value of  $\epsilon$  is fixed to maintain a Reynolds number of 50 based on the eddy

viscosity, the streamwise grid spacing, and the inflow velocity.

STREMR uses a staggered marker-and-cell grid, with normal velocity components defined on the cell faces and pressures defined at the cell centers. This finite-volume grid arrangement allows the pressure to be computed from a Poisson equation. Since the normal velocity components are known (or calculated) in advance for all boundaries, the derivative of pressure normal to the boundaries can be set to zero. STREMR uses a variant of the MacCormack predictor-corrector scheme (MacCormack 1969; Bernard 1989, 1992) to solve Equation 2, and a single-step upwind scheme (Anderson, Tannehill, and Pletcher 1984) to solve Equations 11 and 12. Steady-state solutions are achieved by marching forward in time, with potential flow or some other mass-conserving flow used for the initial velocity, and small uniform values specified for the initial turbulence quantities.

For open channels, the water surface is assumed to be a rigid lid. With this constraint, the pressure computed for any given cell is equal to the displacement that would otherwise occur for a free surface at that location. This assumption limits the applicability of STREMR to subcritical flow. If the streamwise variations in channel width or depth are very gentle, and if there are no obstacles (piers, dikes, or islands) in the flow, then the code may be valid at Froude numbers as high as 0.6 or 0.7. Otherwise, the upper limit on the Froude number is 0.5.

PART III: SECONDARY FLOW CORRECTION

To obtain an approximation for  $\tau_s$  without a fully 3-D discretization, one first needs an equation for production, transport, and dissipation of streamwise vorticity. Qualitative arguments dictate the form of this equation, whose empirical coefficients (free parameters) have to be adjusted to make model predictions fit experimental data. If the SFC is to be quantitatively useful in general, then coefficients obtained for one channel should yield acceptable predictions for other channels with different depth, curvature, and bottom friction.

Let  $z$  be the vertical direction, with the water surface at  $z = h/2$  and the channel bottom at  $z = -h/2$ ; and let  $\underline{u}'(z)$  be a  $z$ -dependent perturbation of the depth-averaged velocity  $\underline{u}$ . By definition,  $\underline{u}'(z)$  must satisfy the constraint

$$\int_{-h/2}^{h/2} \underline{u}'(z) dz = 0 \quad (14)$$

If  $\underline{u} + \underline{u}'$  is substituted for  $\underline{u}$  when deriving the depth-averaged momentum equation, then there is a perturbation  $h\tau'$  of the depth-integrated shear stress  $h\tau_{12}$  in the vertical plane (elevation view), given by

$$h\tau' = -\rho \int_{-h/2}^{h/2} u'v' dz \quad (15)$$

where  $u'$  and  $v'$  are the  $x$ - and  $y$ -components of  $\underline{u}'$ .

Equation 14 requires that the depth integral be zero for both  $u'$  and  $v'$ , but not for their product  $u'v'$ . The simplest functional forms that make the integral of  $\underline{u}'$  zero, without necessarily making the integral of  $u'v'$  zero, are the expressions

$$u' = \omega_2 z \quad (16)$$

$$v' = -\omega_1 z \quad (17)$$

where  $\omega_1$  and  $\omega_2$  are the  $x$ - and  $y$ -components of depth-averaged vorticity.

If the primary flow is in the  $x$ -direction, so that  $v = 0$  but  $u \neq 0$ , then  $\omega_1$  is the streamwise vorticity associated with out-of-plane (secondary)

motion of fluid particles in the (primary) xz-plane. The other vorticity component  $\omega_2$  is perpendicular to  $\omega_1$  and characterizes the z-dependence of  $u'(z)$  in the xz plane. Substitution of Equations 16 and 17 into Equation 15 produces

$$\tau' = \frac{\rho h^2 \omega_1 \omega_2}{12} \quad (18)$$

The dominant term in the empirical relation used by Johannesson and Parker (1989, a and b) indicates that a first approximation for  $\omega_2$  is

$$\omega_2 \approx C_2 \frac{u \sqrt{C_f}}{h} \quad (19)$$

where  $C_2$  is a constant of proportionality. Equations 18 and 19 now give way to

$$\tau' = \frac{C_2 \omega_1}{12} \rho h u \sqrt{C_f} \quad (20)$$

Assuming that Equation 19 holds for streamwise velocity in any direction, then  $\omega_1$  can be equated with the streamwise vorticity  $\omega_s$  and  $\tau'$  can be equated with  $\tau_s$ . It is convenient to express the latter as

$$\tau_s = \rho h \Omega |\underline{u}| \sqrt{C_f} \quad (21)$$

where

$$\Omega = \frac{C_2 \omega_s}{12} \quad (22)$$

With  $C_f$  given by Equation 7, only  $\Omega$  remains to be determined in the expression for  $\tau_s$ .

Consider a vertical column of water in a flow that has (lateral) radius of curvature  $r$  in the (plan view) xy-plane. Let the streamwise velocity  $u_s(z)$  be given by

$$u_s(z) = |\underline{u}| \left( 1 + C_2 \frac{z}{h} \sqrt{C_f} \right) \quad (23)$$

with the outward radial velocity  $u_r(z)$  given by

$$u_r(z) = \omega_s z \quad (24)$$

At any vertical position  $z$ , there is a centrifugal (outward radial)

acceleration  $u_s^2/r$  due to curvature. This creates an out-of-plane angular acceleration  $zu_s^2/r$  along the column, which in turn produces the secondary flow.

To satisfy the no-slip condition at the very bottom of the column, the radial velocity  $u_r$  must go from  $\omega_s h/2$  to zero in some small vertical distance  $\delta$ . Assuming there is a vertical eddy viscosity proportional to  $C_f^{1/2} |\underline{u}| \delta$ , then there must be a shear stress at the bottom, roughly proportional to  $h C_f^{1/2} \rho \omega_s |\underline{u}|$ , which opposes out-of-plane rotation. This stress is negligible at distances greater than  $\delta$  from the bottom. Conservation of angular momentum for the entire column requires that

$$\rho \frac{d}{dt} \int_{-h/2}^{h/2} \omega_s z^2 dz = -\frac{\rho}{2} C_1 h^2 \omega_s |\underline{u}| \sqrt{C_f} + \rho \int_{-h/2}^{h/2} \frac{u_s^2}{r} z dz \quad (25)$$

where  $C_1$  is a constant of proportionality.

When the integration is carried out with Equation 23 substituted for  $u_s$ , Equation 25 gives way to

$$\frac{d\omega_s}{dt} = 2 C_2 \sqrt{C_f} \frac{|\underline{u}|^2}{rh} - 6 C_1 \sqrt{C_f} \omega_s \frac{|\underline{u}|}{h} \quad (26)$$

After Equations 22 and 26 are combined, the equation for streamwise vorticity reduces to

$$\frac{d\Omega}{dt} = \frac{C_2^2}{6} \sqrt{C_f} \frac{|\underline{u}|^2}{rh} - 6 C_1 \sqrt{C_f} \Omega \frac{|\underline{u}|}{h} \quad (27)$$

Equation 27 asserts that  $d\Omega/dt$  depends upon velocity, depth, bottom friction, radius of curvature, and two free parameters,  $C_1$  and  $C_2$ . The functional form comes from the assumed  $z$ -dependence of the streamwise and out-of-plane velocities, and from the imposition of centrifugal and frictional forces on a vertical column of water. In this context, the coefficients  $C_1$  and  $C_2$  are universal constants that have to be determined from experimental data.

Since Equation 27 is based solely on qualitative arguments, the grouping of coefficients is arbitrary. The important thing is that the equation contains two free parameters. Furthermore, in addition to production and dissipation, one also expects some lateral diffusion of  $\Omega$  caused by small-scale turbulence. Based on these considerations, the following is proposed as

the governing equation for streamwise vorticity:

$$\frac{\partial \Omega}{\partial t} + \underline{u} \cdot \nabla \Omega = \frac{A_s \sqrt{C_f} |\underline{u}|^2}{rh(1 + 9h^2/r^2)} - D_s \sqrt{C_f} \Omega \frac{|\underline{u}|}{h} + \frac{1}{h} \nabla \cdot (\nu h \nabla \Omega) \quad (28)$$

This is the secondary flow equation that is used in STREMR. The coefficients  $C_1$  and  $C_2$  have been replaced for convenience by  $A_s$  and  $D_s$ , and the production term has been reduced by an extra factor  $(1 + 9h^2/r^2)$  in the denominator. The latter modification leaves the production term unchanged as long as  $h/r \ll 1$ . Otherwise, the arguments supporting Equation 27 are invalid, and production of  $\Omega$  is automatically forced to zero when  $h/r$  becomes large.

With the governing equation established, only the question of initial and boundary conditions remains. The initial value of  $\Omega$  is taken to be zero everywhere, and  $\Omega$  is fixed at zero for all time on inlets. The normal derivative in the diffusion term is set to zero on outlets and sidewalls. Since the secondary flow must vanish on the sidewalls, production of  $\Omega$  is reduced by one half in grid cells adjacent to the sidewalls. Otherwise, STREMR discretizes and solves Equation 28 in the same manner as Equations 11 and 12.

## PART IV: RESULTS

The secondary flow model (Part III, Equation 28) contains two empirical coefficients ( $A_s$  and  $D_s$ ) whose values must be established by trial-and-error comparison of predicted and measured velocities. If the SFC is genuinely reliable, then the values of  $A_s$  and  $D_s$  for one channel and one flow condition should give, without further adjustment, satisfactory predictions for other channels and other flow conditions. It will now be demonstrated that coefficients tuned for a single 270-deg\* bendway can indeed be used to predict velocity distributions for two dissimilar channels with multiple bendways. That does not guarantee that the particular values used for  $A_s$  and  $D_s$  will be the best for all channels of interest, but it is a crucial step toward validating the SFC. If STREMR were able to reproduce only the bendway data for which  $A_s$  and  $D_s$  were specifically tuned, then it would indicate that something important is still missing in the secondary flow model.

### 270-Deg Bendway

The benchmark for establishing preliminary values of  $A_s$  and  $D_s$  is a 270-deg bendway with a vertical inner sidewall and a sloped outer bank. Figure 1 shows the wetted cross section, with the STREMR grid (387 cells long  $\times$  32 cells wide) superposed on the plan view. All linear dimensions are given in feet. For the test under consideration (Hicks, Jin, and Steffler 1990), the flow rate is 0.83 cfs and the Manning coefficient is 0.010, which makes  $C_f = 0.0025$  in the middle of the channel. The ratio of depth to radius of curvature ( $h/r$ ) varies from 0.016 at the toe of the outer bank, to 0.021 at the inner sidewall. The outer bank was modeled in STREMR with four one-cell-wide stair steps. The inflow velocity was assumed uniform except on the outer bank, where it was specified as a linear function of distance from the water's edge. After considerable trial and error, the SFC coefficients were set at  $A_s = 5$  and  $D_s = 1/2$ .

Figure 2 shows velocity vectors, computed with and without the SFC, at stations along the full length of the channel. Figure 3 compares predicted

---

\* A table of factors for converting non-SI units of measurement to SI (metric) units is presented on page 3.

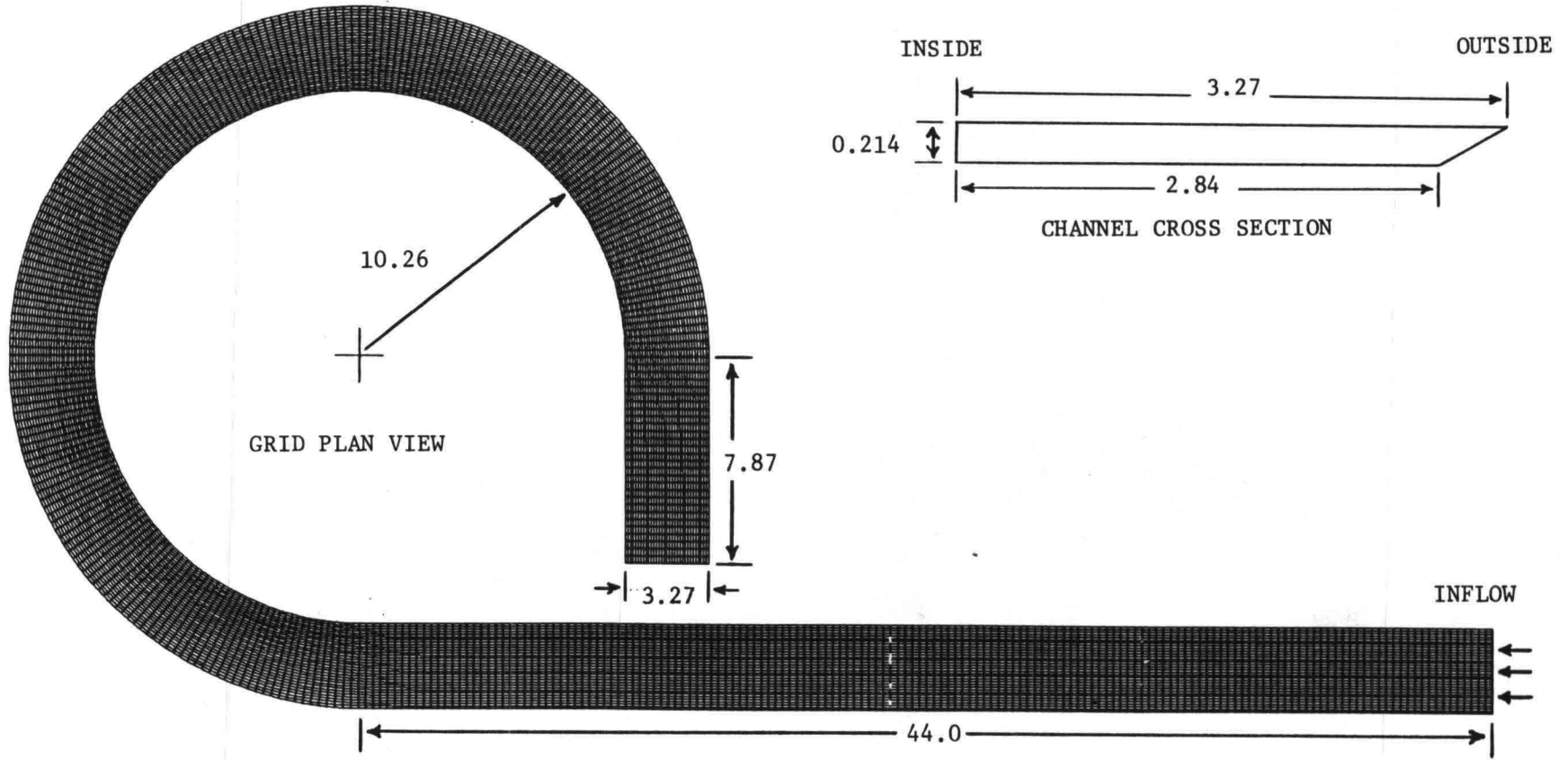
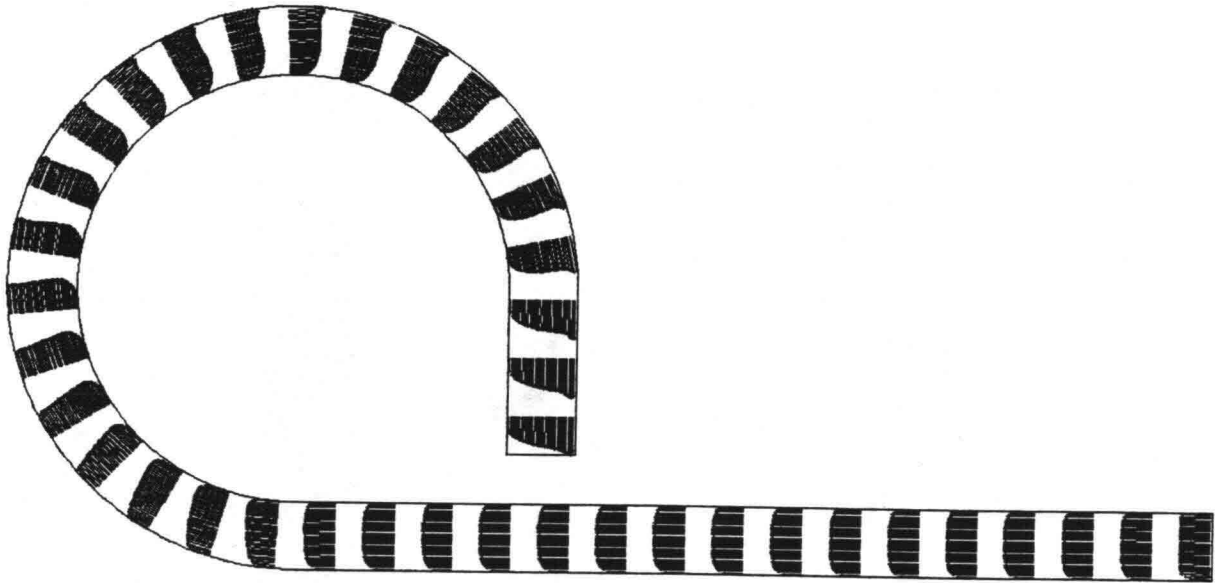
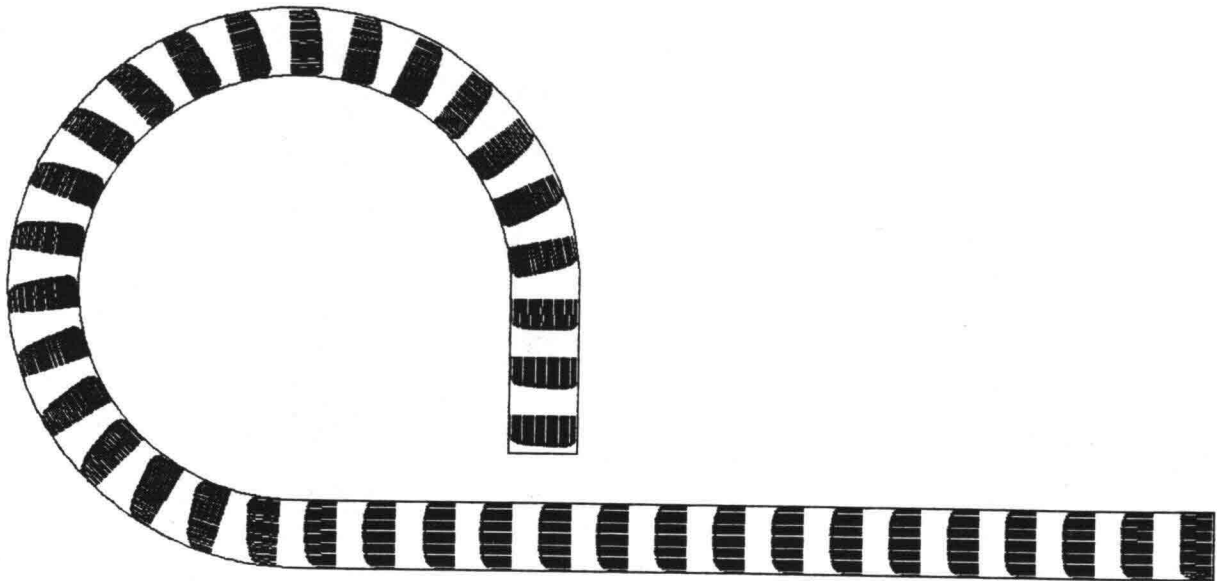


Figure 1. Grid plan view and channel cross section for 270-deg bendway

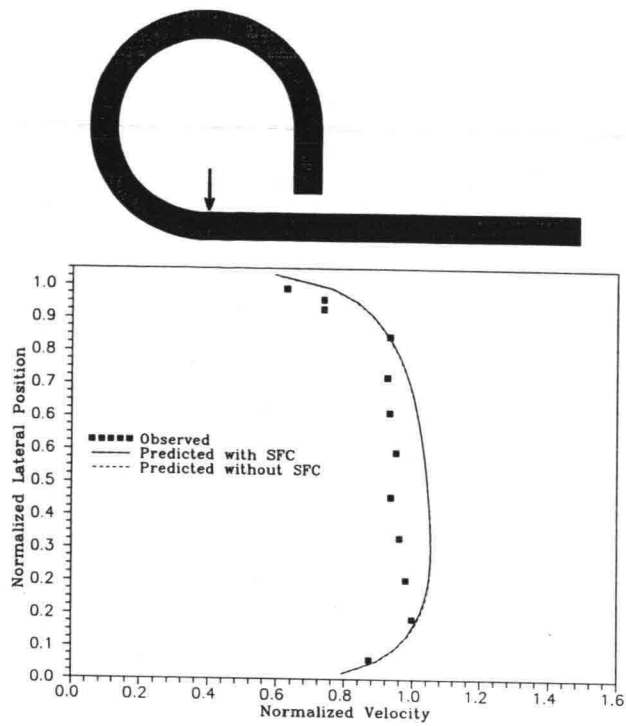


a. Predicted with SFC

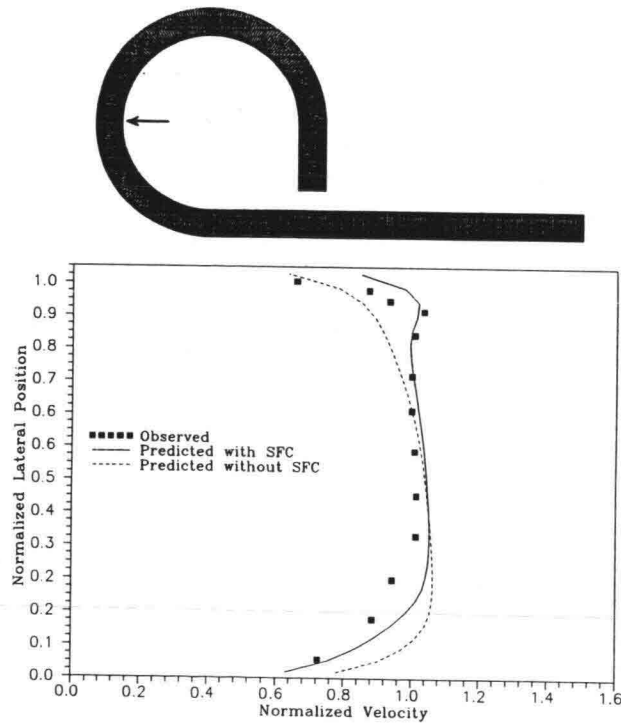


b. Predicted without SFC

Figure 2. Computed velocity vectors for 270-deg bendway

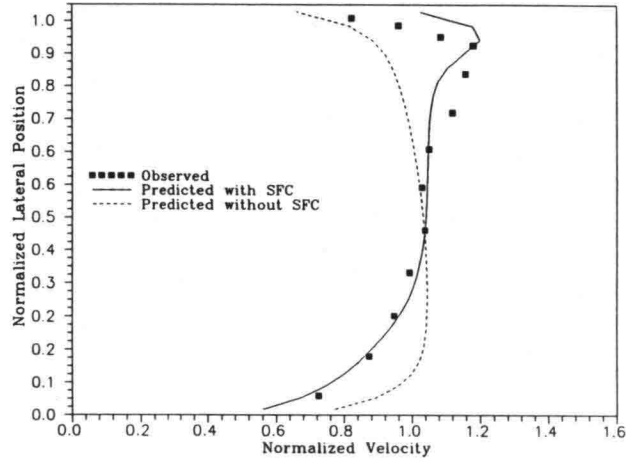
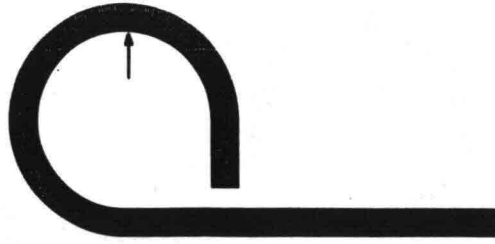


a. Station 1

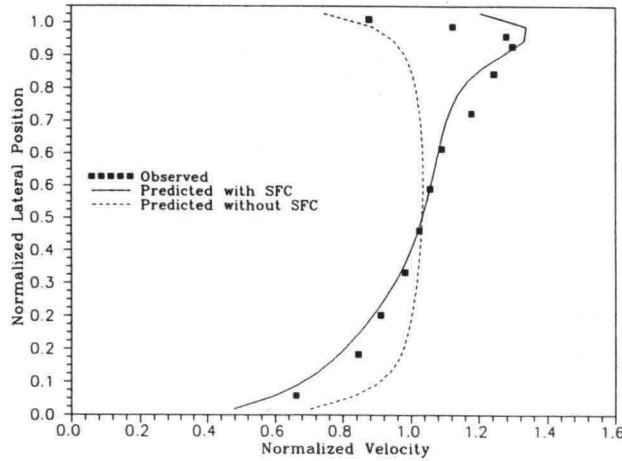
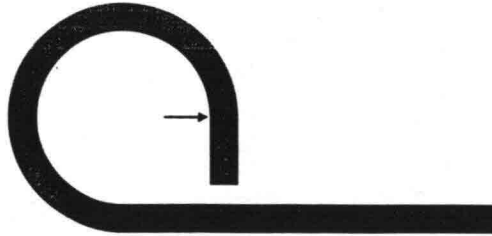


b. Station 2

Figure 3. Depth-averaged velocity for the 270-deg bendway (Continued)



c. Station 3



d. Station 4

Figure 3. (Concluded)

and observed velocities at four individual stations (0, 90, 180, and 270 deg). Normalized velocity is defined to be local depth-averaged velocity divided by average velocity for the channel cross section. Normalized lateral position is radial distance from the inner sidewall divided by cross-channel width of the water surface. For each station, a plan view of the channel is provided with an arrow that indicates the location of the data station along the inner sidewall of the bendway. The velocity profiles are shown as they would be seen by an observer looking in the direction of the arrow.

The SFC/STREMR velocity profiles reproduce the observed profiles well except on the outer bank, where the computed bottom resistance is consistently too low. The underprediction also occurs in straight channels, and it indicates the need for some modification of Equation 7 in response to bottom slope. Finer discretization (more grid lines concentrated on the bank) does not eliminate the problem. It remains to be seen whether this deficiency can be cured without using a fully 3-D numerical model. Otherwise, the SFC (with its tuned coefficients) does a good job of making STREMR predictions match the test data.

Without the SFC, the highest velocity remains near the inside, and the computed profiles bear little resemblance to the observed profiles downstream of the bend entrance (Station 1). In contrast, the SFC causes high velocity to migrate to the outside because of the production term in Equation 28, which becomes nonzero whenever  $h/r$  is nonzero. The production term returns to zero in straight sections, leaving only the dissipation term, which gradually kills the secondary flow. If there is a reversal in curvature, there will be a migration of high velocity toward the opposite side of the channel. The coefficients  $A_s$  and  $D_s$  determine the precise rates of migration, dissipation, and reversal.

#### Channel Bend Facility

Maynard\* has made detailed velocity measurements in an S-shaped flume called the Channel Bend Facility (CBF). The CBF entails two bends with a reversal in curvature and a trapezoidal cross section, and it represents a

---

\* Unpublished test data provided by S. T. Maynard, Research Hydraulic Engineer, August 1987, US Army Engineer Waterways Experiment Station, Vicksburg, MS.

considerable departure from the geometry of the 270-deg bendway. Figure 4 shows the wetted cross section, with the STREMR grid (121 cells long  $\times$  46 cells wide) superposed on the plan view. All linear dimensions are given in feet. For the test under consideration,\* the flow rate is 6.75 cfs and the Manning coefficient is 0.02, which makes  $C_f = 0.0075$  in the middle of the channel. The ratio of depth to radius of curvature ( $h/r$ ) varies in the bends from 0.018 at the toe of the outer bank, to 0.025 at the toe of the inner bank. The banks were discretized in STREMR with five one-cell-wide stair steps on each side of the channel. The inflow velocity was assumed uniform except on the banks, where it was specified as a linear function of distance from the water's edge. The SFC coefficients were set at  $A_s = 5$  and  $D_s = 1/2$ .

Figure 5 shows velocity vectors, computed with and without the SFC, at stations along the full length of the CBF. Figure 6 compares predicted and observed velocities at five individual stations, whose locations are indicated by the arrow on each included plan view. As before, the velocity profiles are shown as they would be seen by an observer looking in the direction of the arrow. Normalized velocity is defined to be local depth-averaged velocity divided by average velocity for the channel cross section. Normalized lateral position is radial distance from the inner water surface (indicated by the tip of the arrow) divided by cross-channel width of the water surface.

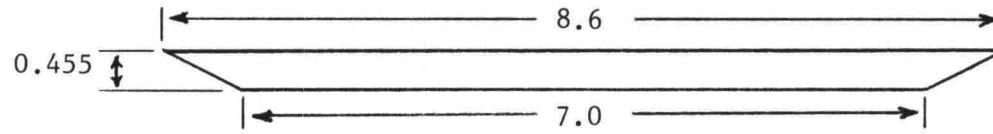
The agreement between the SFC/STREMR predictions and the observed velocity profiles is at least as good for the CBF as it was for the 270-deg bendway. Here the average value of  $h/r$  is only slightly greater, but the value of  $C_f$  is three times greater here than that for the 270-deg bend. This lends support to the proposed influence of  $C_f$  in the SFC.

#### Riprap Test Facility

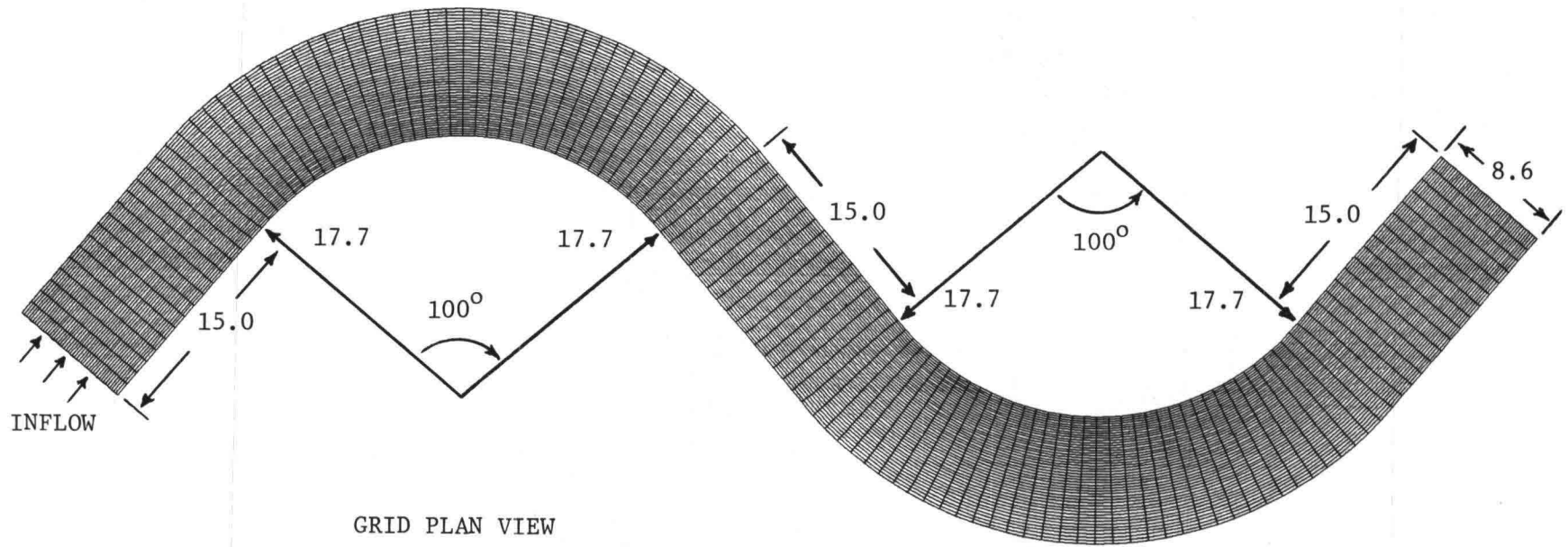
The Riprap Test Facility (RTF) is a trapezoidal channel with four bends and two reversals in curvature. Maynard\* has conducted a test in the RTF with a flow rate of 49.5 cfs and a Manning coefficient of 0.026. Figure 7 shows the wetted cross section, with the STREMR grid (391 cells long  $\times$  36 cells

---

\* Unpublished test data provided by S. T. Maynard, Research Hydraulic Engineer, August 1987, US Army Engineer Waterways Experiment Station, Vicksburg, MS.

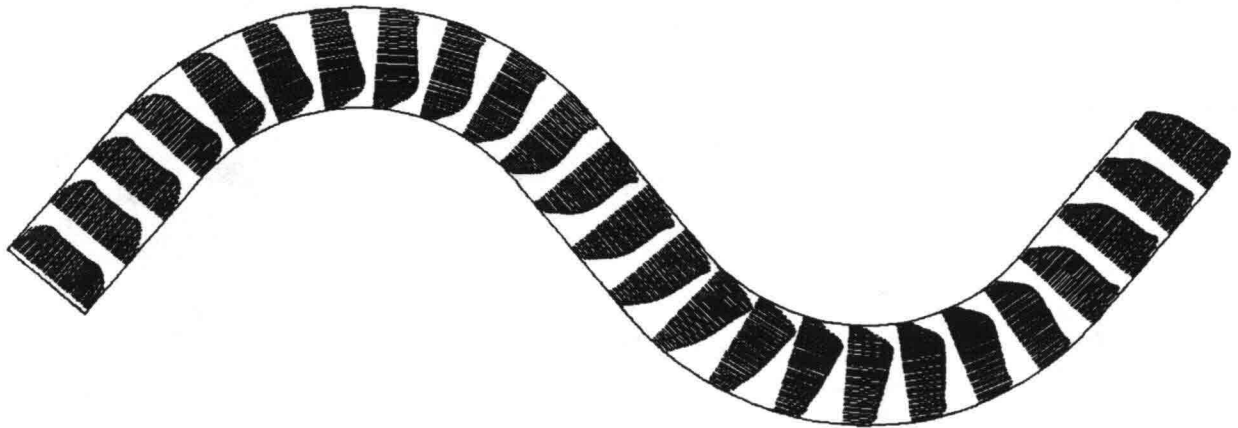


CHANNEL CROSS SECTION

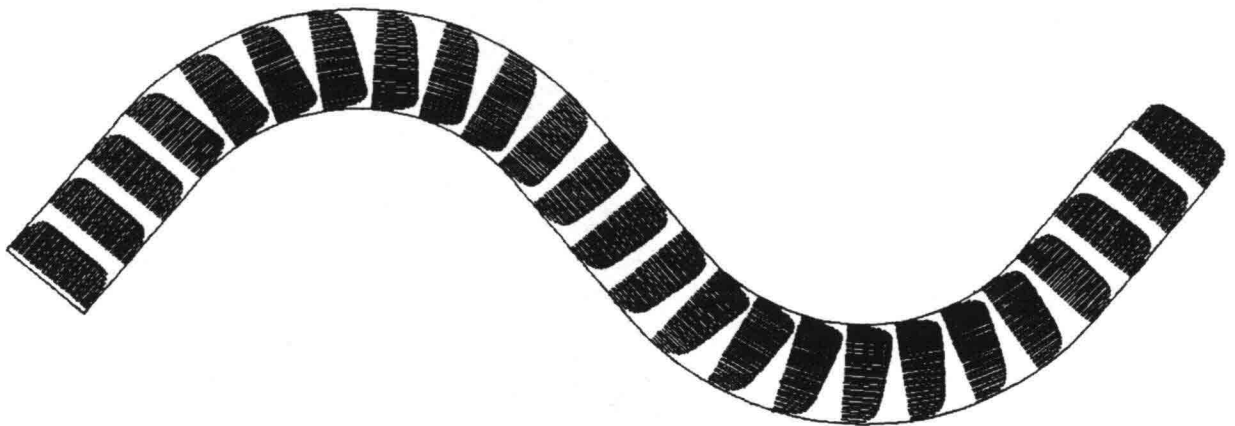


GRID PLAN VIEW

Figure 4. Grid plan view and channel cross section for CBF

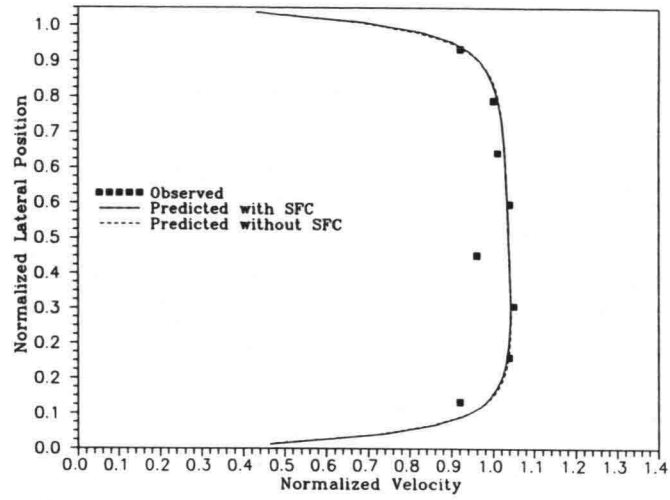
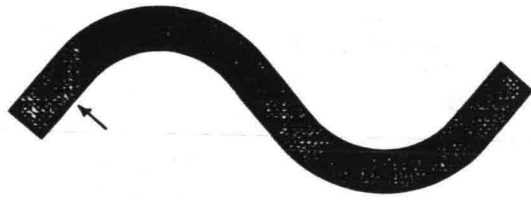


a. Predicted with SFC

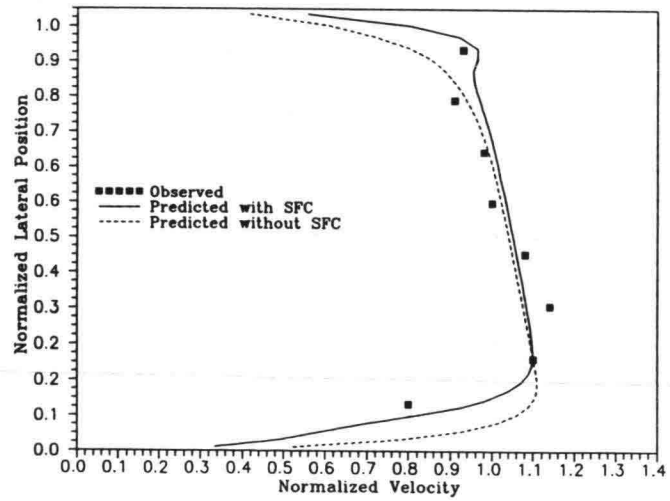


b. Predicted without SFC

Figure 5. Computed velocity vectors for CBF

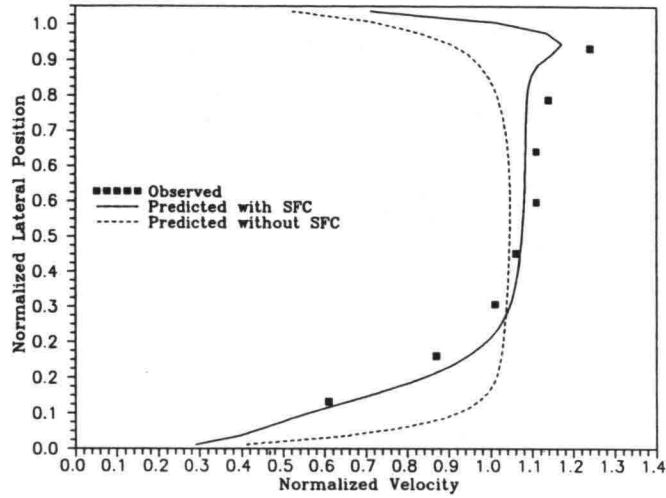
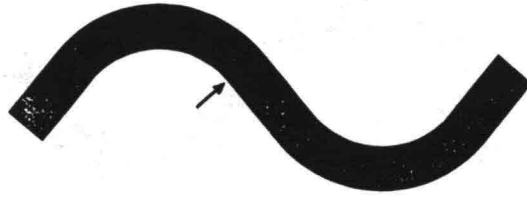


a. Station 1

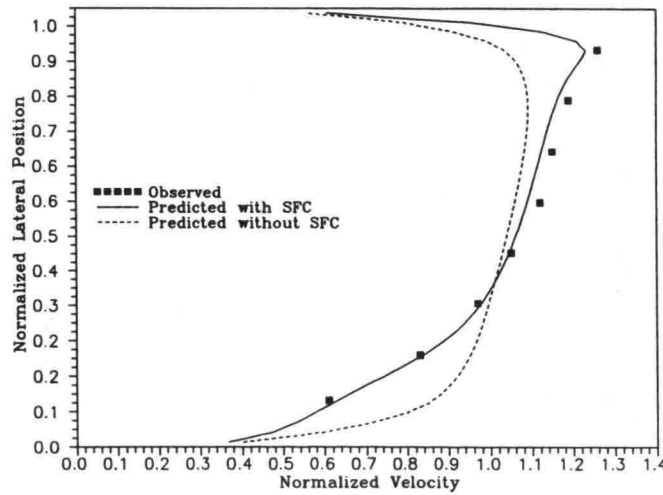


b. Station 2

Figure 6. Depth-averaged velocity for the CBF (Sheet 1 of 3)

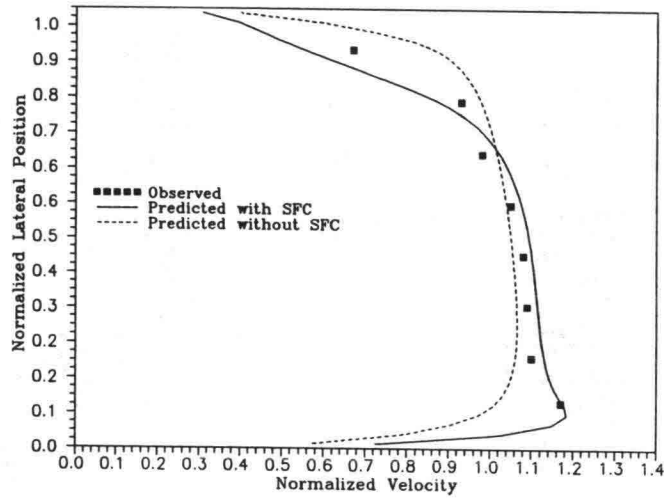


c. Station 3



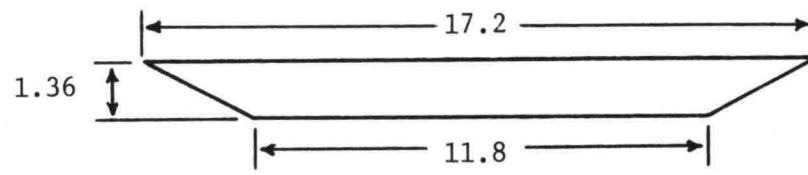
d. Station 4

Figure 6. (Sheet 2 of 3)

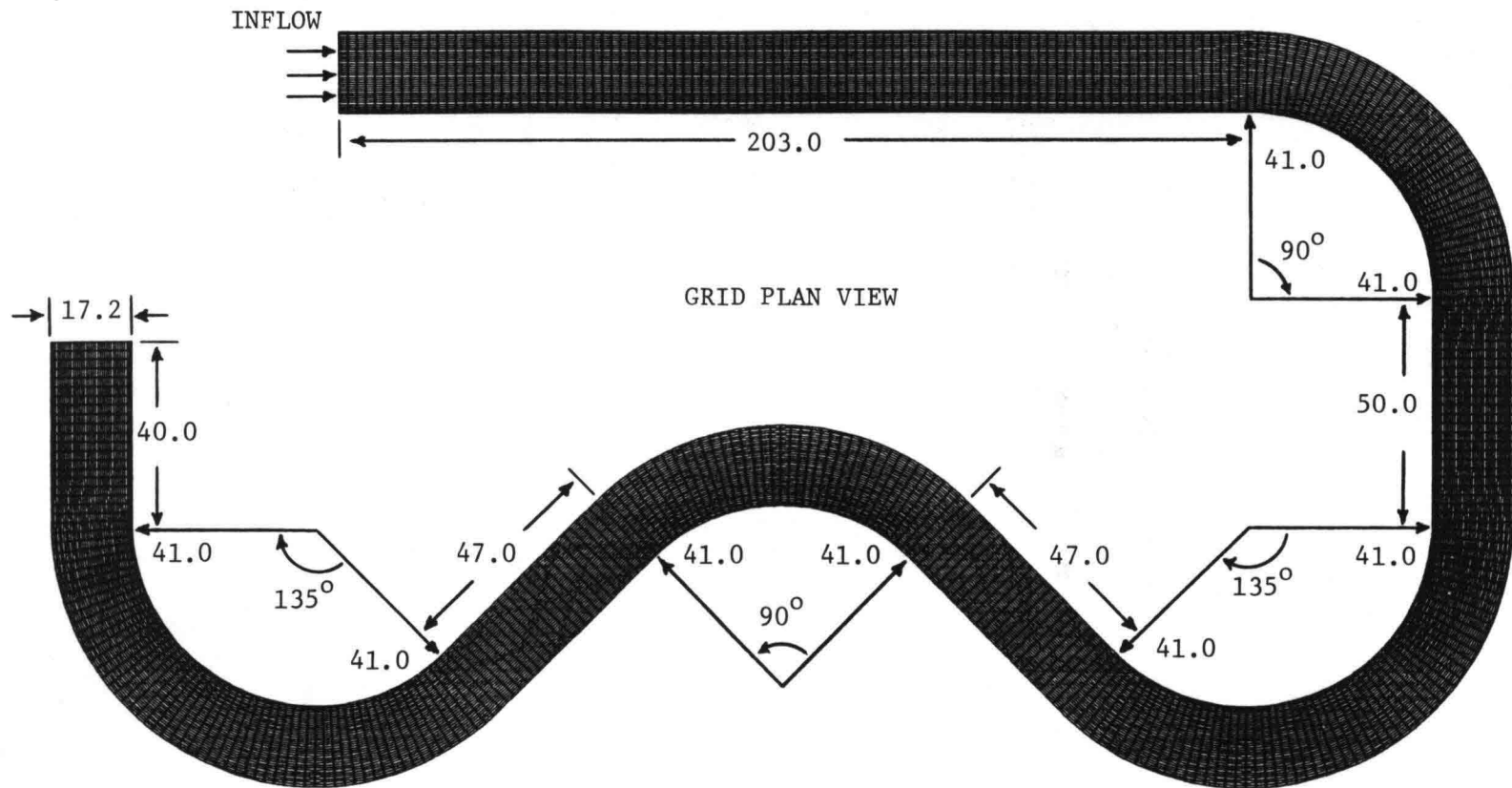


e. Station 5

Figure 6. (Sheet 3 of 3)



CHANNEL CROSS SECTION



GRID PLAN VIEW

Figure 7. Grid plan view and channel cross section for RTF

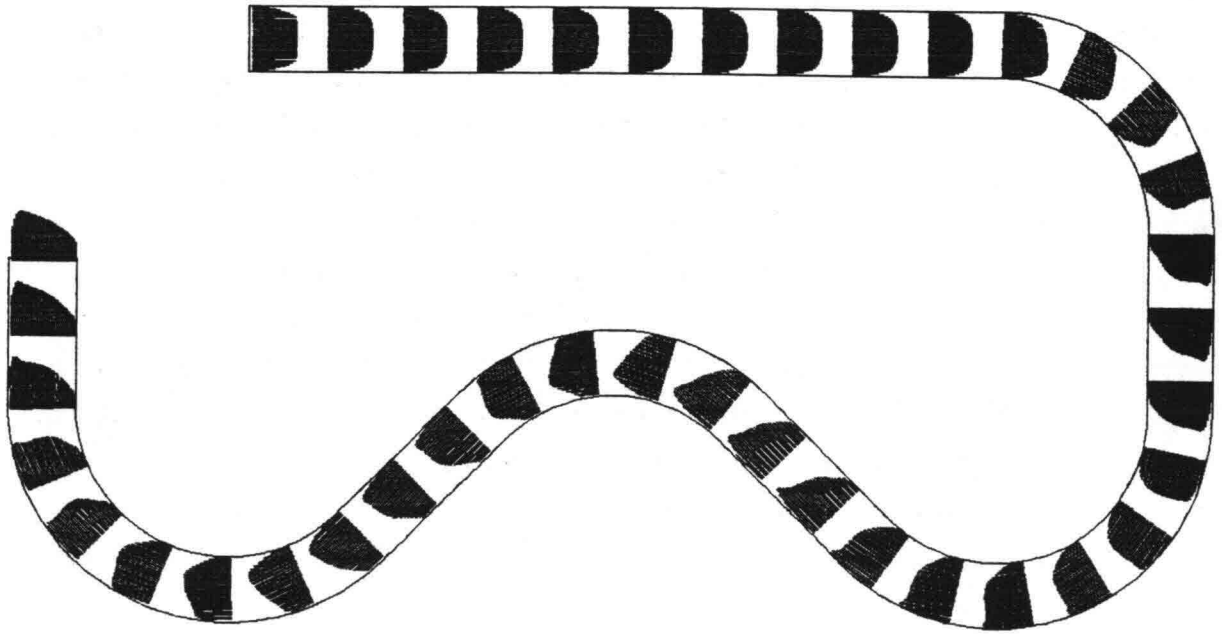
wide) superposed on the plan view. All linear dimensions are given in feet. The value of  $C_f$  is 0.0088 in the middle of the channel, and  $h/r$  varies in the bends from 0.024 at the toe of the outer bank to 0.031 at the toe of the inner bank. The average value of  $h/r$  is about 50 percent greater, and the value of  $C_f$  is 3.5 times greater here than that for the 270-degree bend. The banks were discretized in STREMR with six one-cell-wide stair steps on each side of the channel. The inflow velocity was assumed uniform except on the banks, where it was specified as a linear function of distance from the water's edge. The SFC coefficients were set at  $A_s = 5$  and  $D_s = 1/2$ .

Figure 8 shows velocity vectors, computed with and without the SFC, at stations along the full length of the RTF. Figure 9 compares predicted and observed velocities at 13 individual stations, whose locations are indicated by the arrow on each included plan view. As before, the velocity profiles are shown as they would be seen by an observer looking in the direction of the arrow. Normalized velocity is defined to be local depth-averaged velocity divided by average velocity for the channel cross section. Normalized lateral position is radial distance from the inner water surface (indicated by the tip of the arrow) divided by cross-channel width of the water surface.

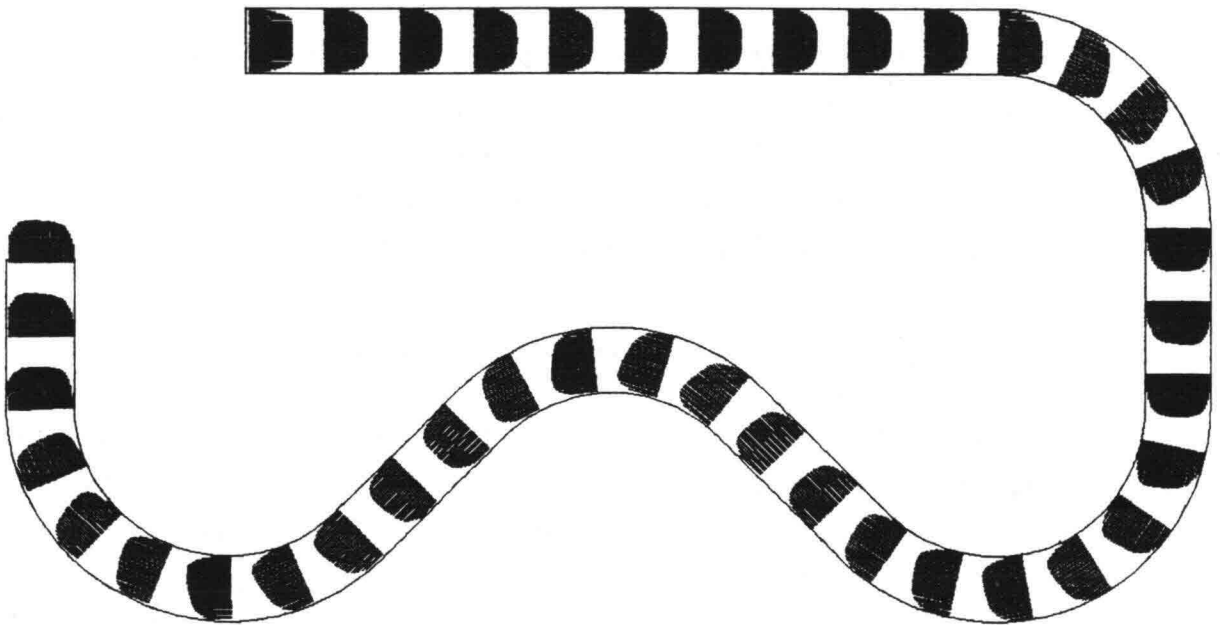
Up to the third bend, the agreement between the SFC/STREMR predictions and the observed velocity profiles is about as good for the RTF as it was for the CBF and the 270-degree bendway. There is some deterioration of accuracy in the third bend (Stations 10 through 12), even though the predictions still follow the observed trends for velocity migration. Accuracy has begun to recover at the entrance to the fourth bend (Station 13).

#### Hypothetical Effect of Bend Angle

Since the SFC (with  $A_s = 5$  and  $D_s = 1/2$ ) yields acceptable predictions for three rather different channels, one expects that it should be no less applicable for minor variations on these configurations. With this in mind, STREMR was used to calculate the hypothetical effect of bend angle for a single-bend channel with the same cross section, radius of curvature, and friction coefficient as the CBF (Figure 4). Specifically, unverified predictions were made for bend angles of 30, 60, 90, and 120 deg, with 20-ft straight sections at the entrance and exit of the bend. The grid spacing was the same as that for the CBF.

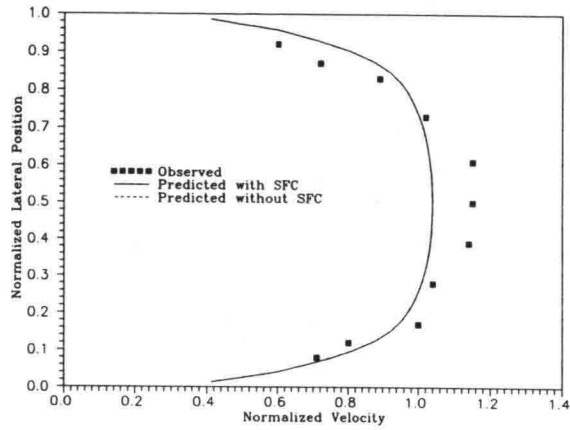
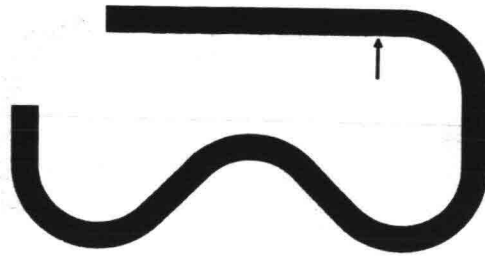


a. Predicted with SFC

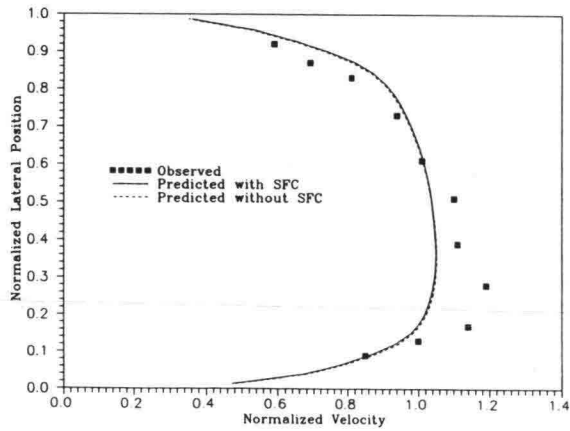
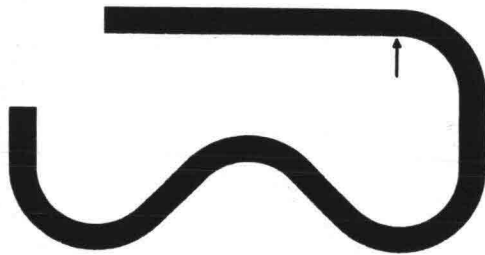


b. Predicted without SFC

Figure 8. Computed velocity vectors for RTF

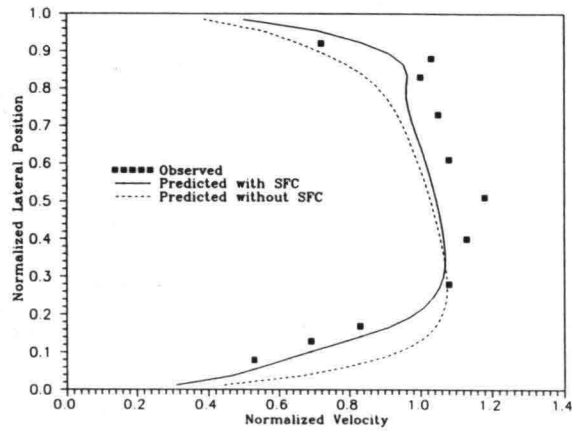
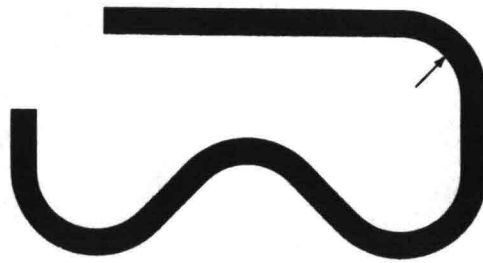


a. Station 1

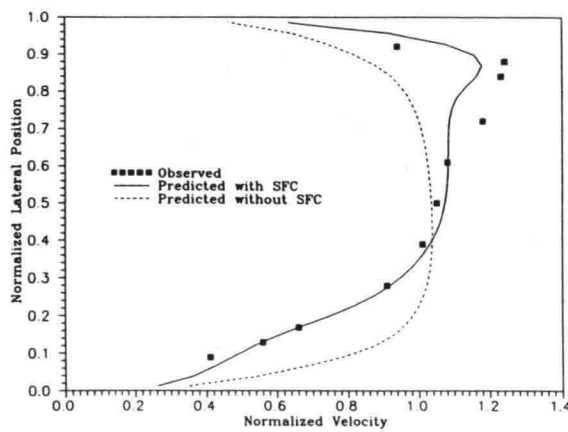
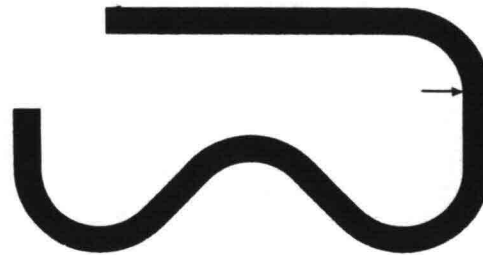


b. Station 2

Figure 9. Depth-averaged velocity for the RTF (Sheet 1 of 7)

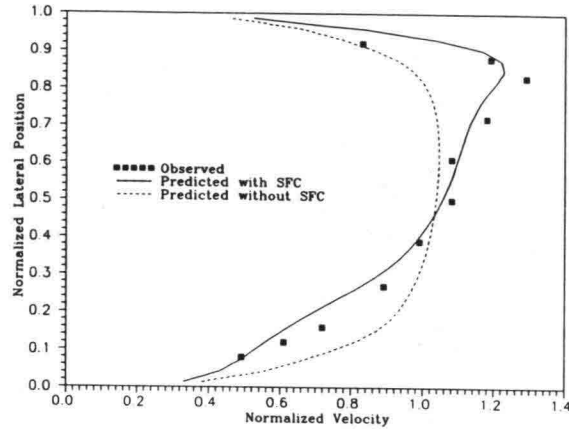
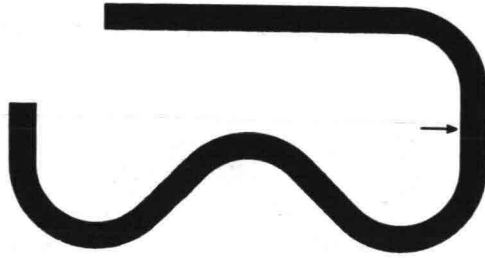


c. Station 3

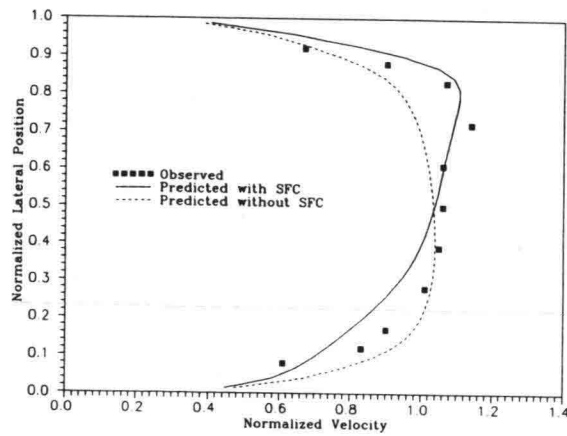
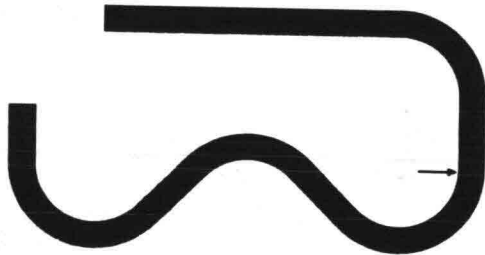


d. Station 4

Figure 9. (Sheet 2 of 7)

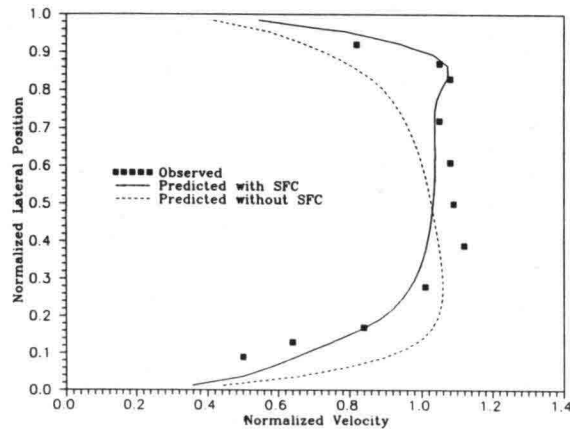
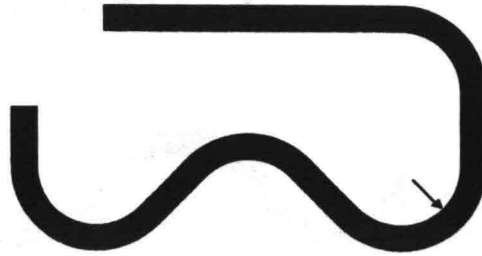


e. Station 5

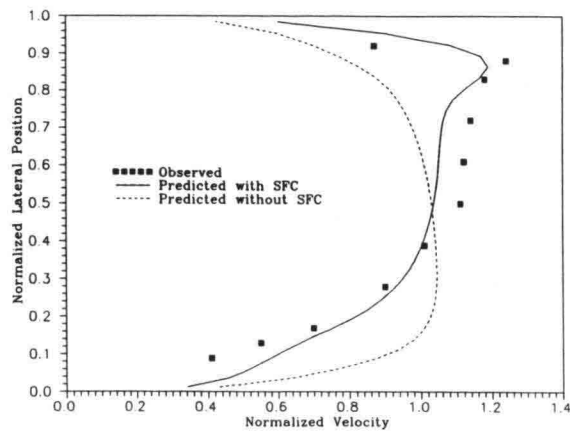
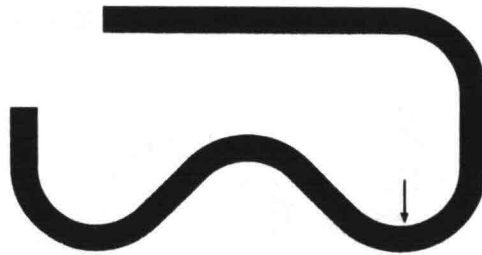


f. Station 6

Figure 9. (Sheet 3 of 7)

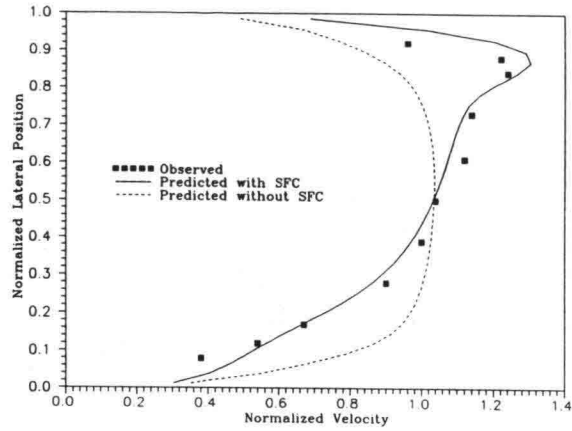
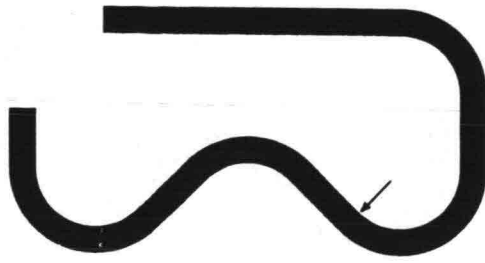


g. Station 7

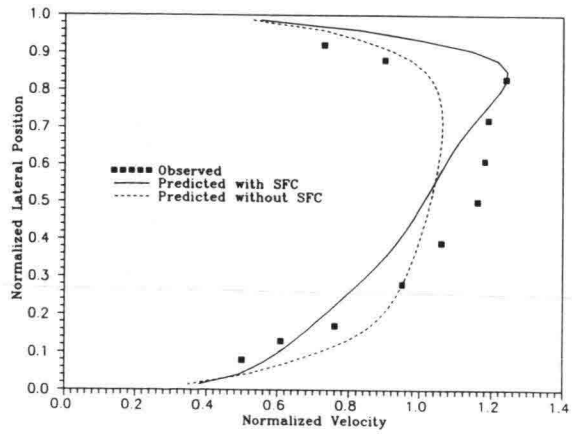
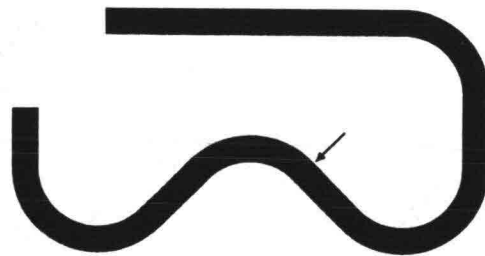


h. Station 8

Figure 9. (Sheet 4 of 7)

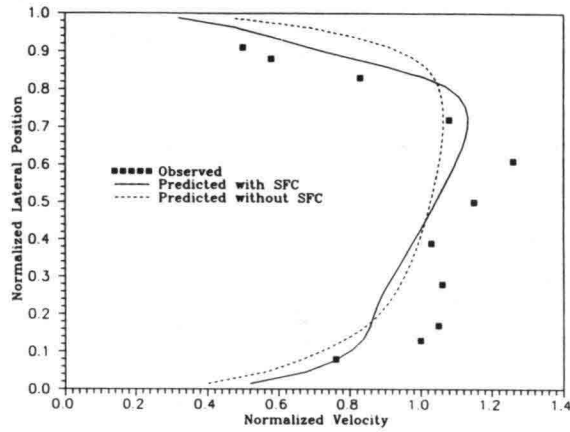
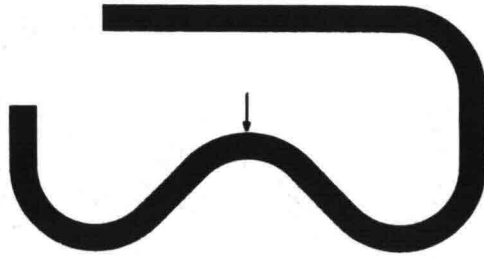


i. Station 9

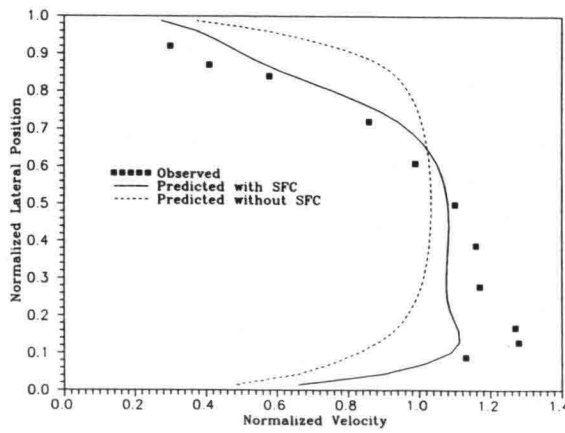
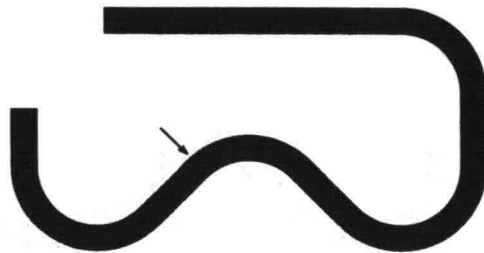


j. Station 10

Figure 9. (Sheet 5 of 7)

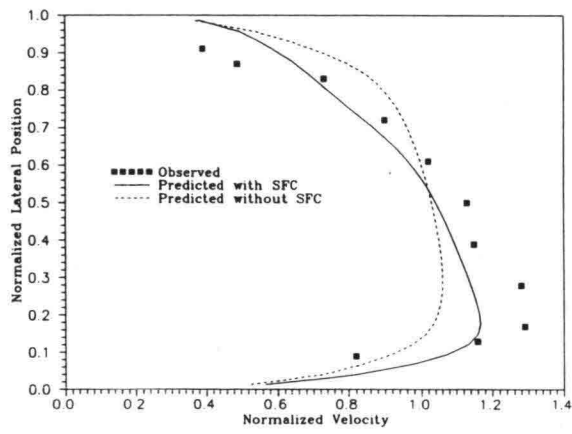
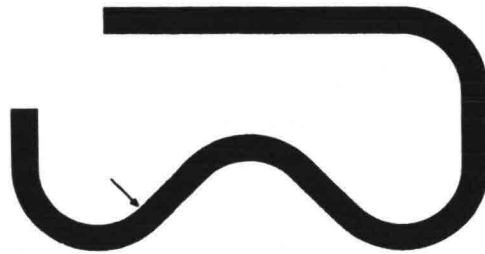


k. Station 11



l. Station 12

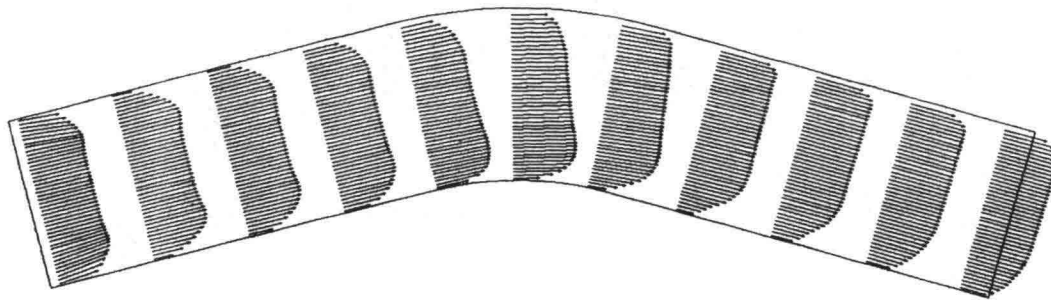
Figure 9. (Sheet 6 of 7)



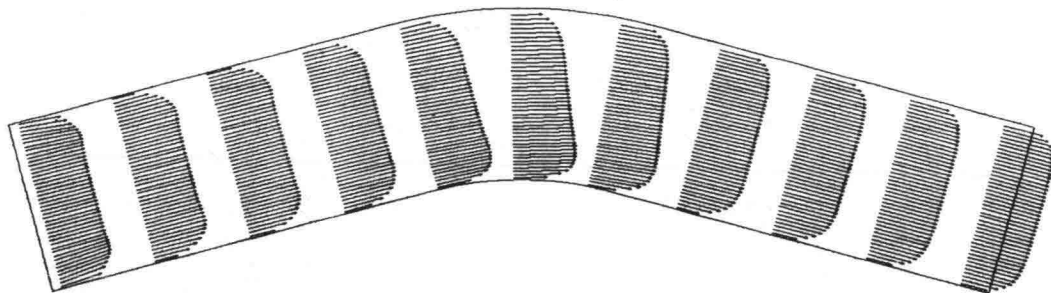
m. Station 13

Figure 9. (Sheet 7 of 7)

Figures 10 through 13 show velocity vectors computed with and without the SFC for the four different bend angles. As in previous cases, the SFC moves the high velocities gradually toward the outside of the bend, where they remain for some distance downstream. Its effect is noticeable even for the 30-deg bend. In contrast, omission of the SFC keeps the high velocity near the insides of the bends.

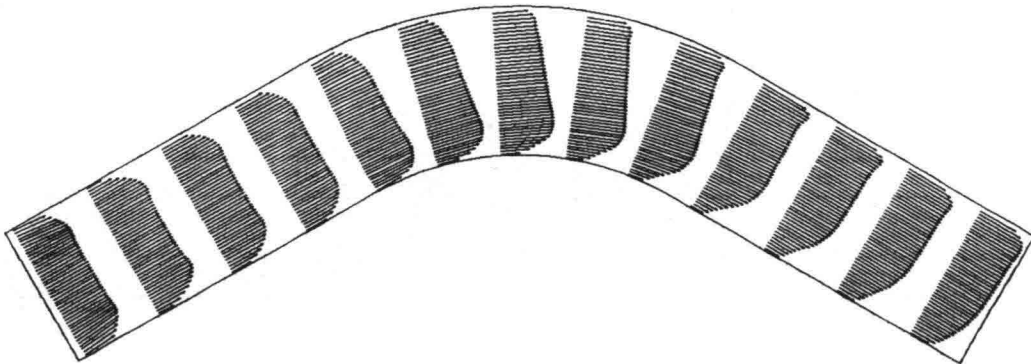


a. Predicted with SFC

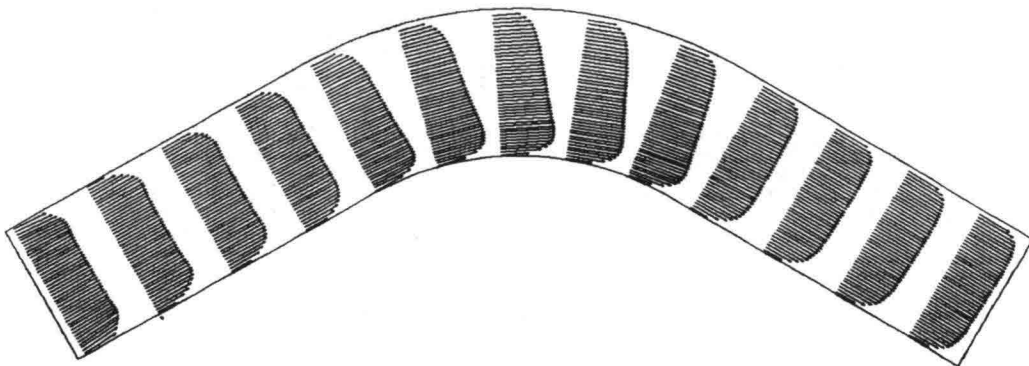


b. Predicted without SFC

Figure 10. Computed velocity vectors for hypothetical 30-deg bend

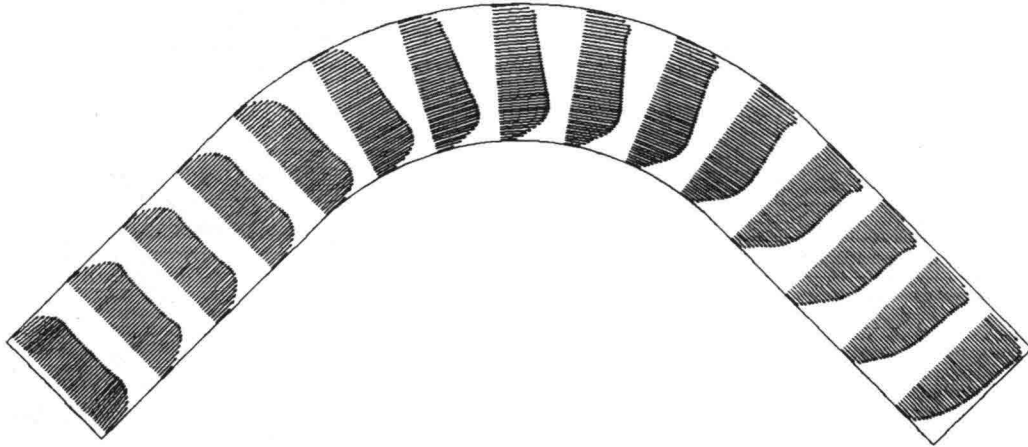


a. Predicted with SFC

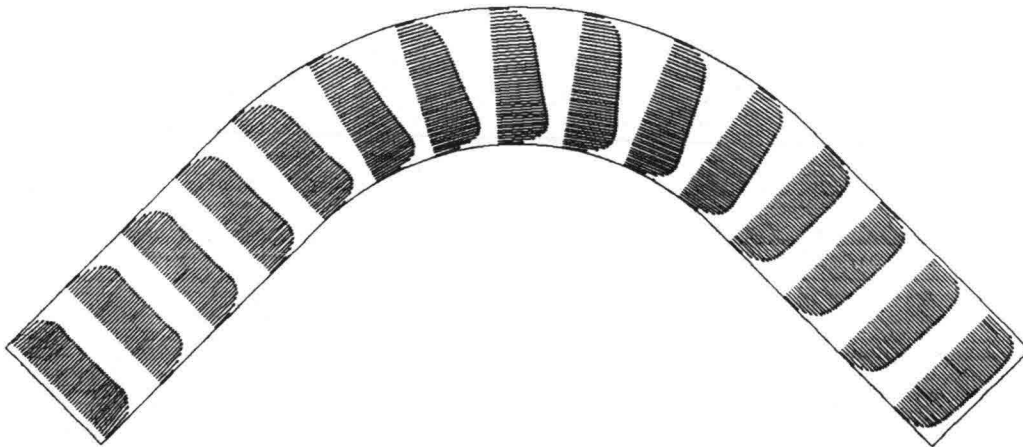


b. Predicted without SFC

Figure 11. Computed velocity vectors for hypothetical 60-deg bend

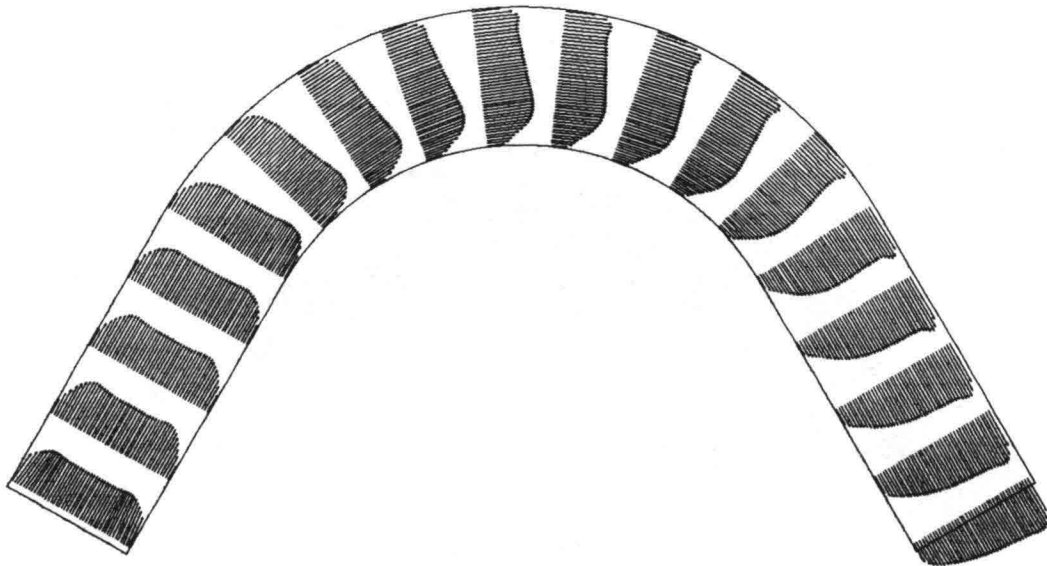


a. Predicted with SFC

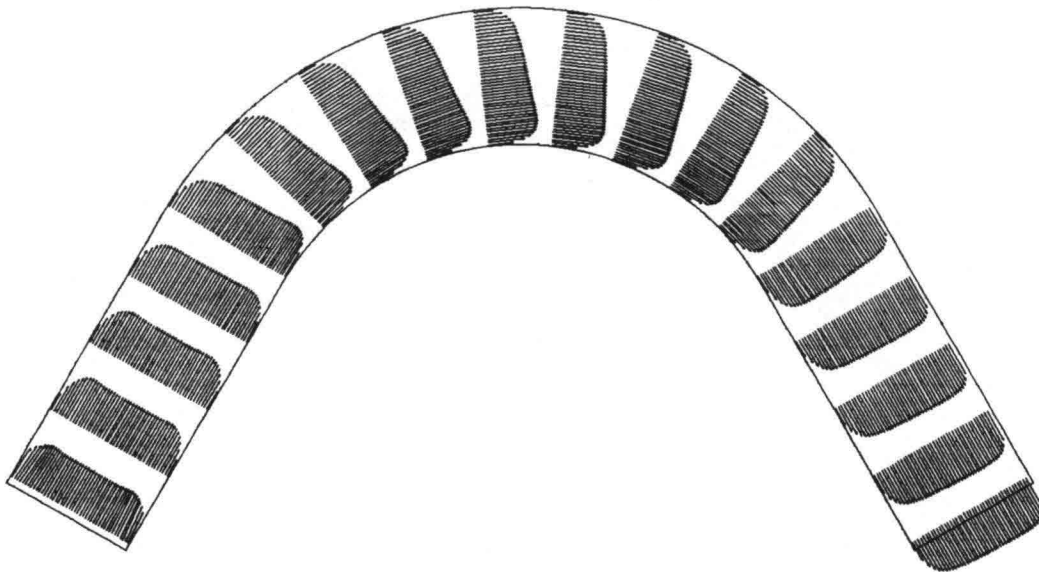


b. Predicted without SFC

Figure 12. Computed velocity vectors for hypothetical 90-deg bend



a. Predicted with SFC



b. Predicted without SFC

Figure 13. Computed velocity vectors for hypothetical 120-deg bend

## PART V: CONCLUSIONS AND RECOMMENDATIONS

An empirical governing equation has been proposed for the secondary flow that gives rise to migration of high velocity toward the outside of channel bends. The secondary flow stems from the interaction between lateral curvature and vertically nonuniform velocity, and it creates an unbalanced force that alters the primary flow. The depth-averaged secondary flow correction (SFC) includes two coefficients ( $A_s$  and  $D_s$ ) whose values have been tuned for agreement between STREMR numerical model predictions and experimental data for a 270-deg bendway. Using the same values for  $A_s$  and  $D_s$ , the SFC yields STREMR predictions with comparable accuracy for the CBF (two bends) and the RTF (four bends), both of which have depth, bottom friction, and radius of curvature different from the 270-deg benchmark.

Results obtained with the SFC are encouraging, since it was not clear in advance that the same values of  $A_s$  and  $D_s$  would render acceptable predictions for more than a single channel configuration. The form of the secondary flow equation ensures proper qualitative behavior, but not necessarily quantitative accuracy. Comparisons of predicted and measured velocities have demonstrated, however, that coefficients tuned for one channel can also be used for others. It appears that the SFC may be used (with  $A_s = 5$  and  $D_s = 1/2$ ) for ratios of depth  $h$  to radius of curvature  $r$  in the range  $0.0 < h/r < 0.04$ , and for friction coefficients in the range  $0.002 < C_f < 0.01$ . It remains to be seen how well the SFC works outside these bounds without changing the values of  $A_s$  and  $D_s$ . To answer the latter question, more tests will be needed for other channels and flow conditions.

## REFERENCES

- Anderson, D. A., Tannehill, J. C., and Pletcher, R. H. 1984. Computational Fluid Mechanics and Heat Transfer. Hemisphere Publishing Corp., McGraw-Hill, New York, pp 88-96.
- Bernard, R. S. 1989 (Mar). "Explicit Numerical Algorithm for Modeling Incompressible Approach Flow," Technical Report REMR-HY-5, US Army Engineer Waterways Experiment Station, Vicksburg, MS.
- \_\_\_\_\_. "STREMR: Numerical Model for Depth-Averaged Incompressible Flow," in preparation, US Army Engineer Waterways Experiment Station, Vicksburg, MS.
- Hicks, F. E., Jin, Y. C., and Steffler, P. M. 1990. "Flow Near Sloped Bank in Curved Channel," Journal of Hydraulic Engineering, Vol. 116, No. 1, pp 55-70.
- Johannesson, H., and Parker, G. 1989a. "Secondary Flow in Mildly Sinuous Channel," Journal of Hydraulic Engineering, Vol. 115, No. 3, pp 289-308.
- \_\_\_\_\_. 1989b. "Velocity Redistribution in Meandering Rivers," Journal of Hydraulic Engineering, Vol. 115, No. 8, pp 1019-1039.
- Lauder, B. E., and Spalding, D. B. 1974. "The Numerical Calculation of Turbulent Flows," Computer Methods in Applied Mechanics and Engineering, Vol. 3, pp 269-289.
- MacCormack, R. W. 1969. "The Effect of Viscosity in Hypervelocity Impact Cratering," AIAA Paper 69-354, American Institute of Aeronautics and Astronautics, Cincinnati, OH.
- Orlanski, I. 1976. "A Simple Boundary Condition for Unbounded Hyperbolic Flows," Journal of Computational Physics, Vol. 21, pp 251-269.
- Patel, V. C., Rodi, W., and Scheurer, G. 1985. "Turbulence Models for Near-Wall and Low Reynolds Number Flows: A Review," AIAA Journal, Vol. 23, No. 9, pp 1308-1319.

APPENDIX A: NOTATION

$A_s$	Empirical production coefficient for secondary flow
$c_1, c_2, C_v$	Empirical coefficients in turbulence model
$C_1, C_2$	Constants of proportionality
$C_f$	Friction factor given by Manning's equation
$D_s$	Empirical decay coefficient for secondary flow
$h$	Depth
$k$	Turbulence energy
$n$	Manning's coefficient
$\underline{n}$	Unit vector normal to $\underline{u}$
$p$	Pressure
$r$	Lateral radius of curvature
$\underline{S}$	Force arising from secondary flow
$t$	Time
$\underline{T}$	Viscous force arising from the depth-averaged stress tensor
$u$	x-component of $\underline{u}$
$\underline{u}$	Depth-averaged vector velocity
$u'$	x-component of $\underline{u}'$
$u_r$	Radial velocity
$u_r$	Outward radial velocity
$u_s$	Streamwise velocity
$u_s^2/r$	Centrifugal (outward radial) acceleration
$\underline{u}'$	z-dependent perturbation of $\underline{u}$
$v$	y-component of $\underline{u}$
$v'$	y-component of $\underline{u}'$
$\underline{X}$	Resistance force (per unit mass) due to bottom friction
$z$	Vertical position

$zu_s^2/r$	Out-of-plane angular acceleration
$\epsilon$	Turbulence dissipation rate
$\nu$	Eddy viscosity
$\rho$	Density
$\tau_s$	Depth-averaged shear stress
$\omega_1$	x-component of depth-averaged vorticity
$\omega_2$	y-component of depth-averaged vorticity
$\omega_s$	Streamwise component of depth-averaged vorticity
$\Omega$	$\frac{C \omega}{12}$
$\nabla$	Gradient operator

### **Waterways Experiment Station Cataloging-In-Publication Data**

Bernard, Robert S.

Depth-averaged numerical modeling for curved channels / by Robert S. Bernard, Michael L. Schneider ; prepared for Department of the Army, U.S. Army Corps of Engineers.

45 p. : ill. ; 28 cm. — (Technical report ; HL-92-9)

Includes bibliographic references.

1. Channels (Hydraulic engineering) — Mathematical models. 2. Hydraulics — Mathematical models. 3. Turbulence — Mathematical models. 4. Hydrodynamics — Mathematical models. I. Schneider, Michael L. (Michael Lee) II. United States. Army. Corps of Engineers. III. U.S. Army Engineer Waterways Experiment Station. IV. Title. V. Series: Technical report (U.S. Army Engineer Waterways Experiment Station) ; HL-92-9.

TA7 W34 no.HL-92-9

